Supporting Information

Armoring SiO_x with a Conformal LiF Layer to Boost Lithium Storage

Tianxing Kang, Jihua Tan, Xiaocui Li, Jianli Liang, Hui Wang, Dong Shen, Yan Wu, Zhongming Huang, Yang Lu, Zhongqiu Tong, Chun-Sing Lee**

T. Kang, J. Tan, J. Liang, Dr. H. Wang, D. Shen, Y. Wu, Z. Huang, Dr. Z. Tong, Prof. C.-S. Lee
Department of Chemistry
Center of Super-Diamond and Advanced Films (COSDAF)
City University of Hong Kong
Tat Chee Avenue, Kowloon, Hong Kong, China
E-mail: apcslee@cityu.edu.hk

Department of Chemistry
Center of Super-Diamond and Advanced Films (COSDAF)
City University of Hong Kong
Tat Chee Avenue, Kowloon, Hong Kong, China
College of Materials and Metallurgical Engineering, Guizhou Institute of Technology, Guiyang, 550003, Guizhou, China
E-mail: zqtong@163.com

Dr. X. Li, Prof. Y. Lu
Department of Mechanical Engineering
City University of Hong Kong
Tat Chee Avenue, Kowloon, Hong Kong, China

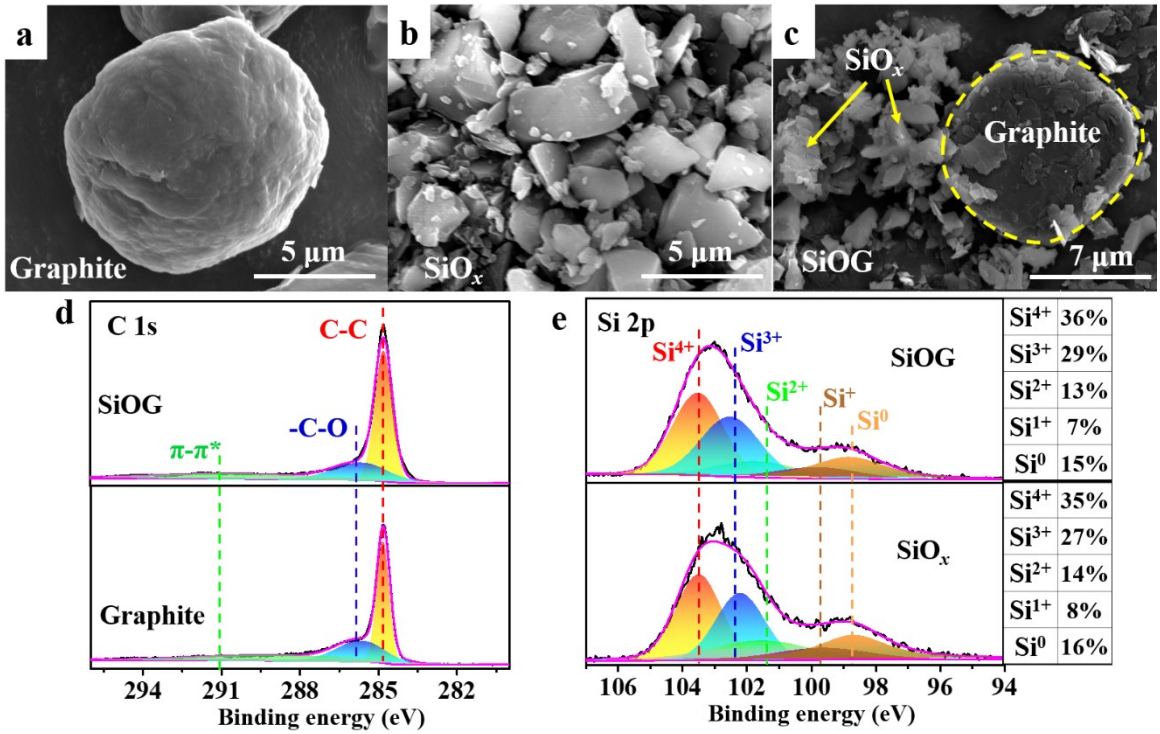

Figure S1. (a, b, c) SEM images of graphite, SiO_x and SiOG. (d) High resolution C 1s XPS spectra of SiOG and graphite. (e) High resolution Si 2p XPS spectra and content of Si in different valence of SiO_x and SiOG.

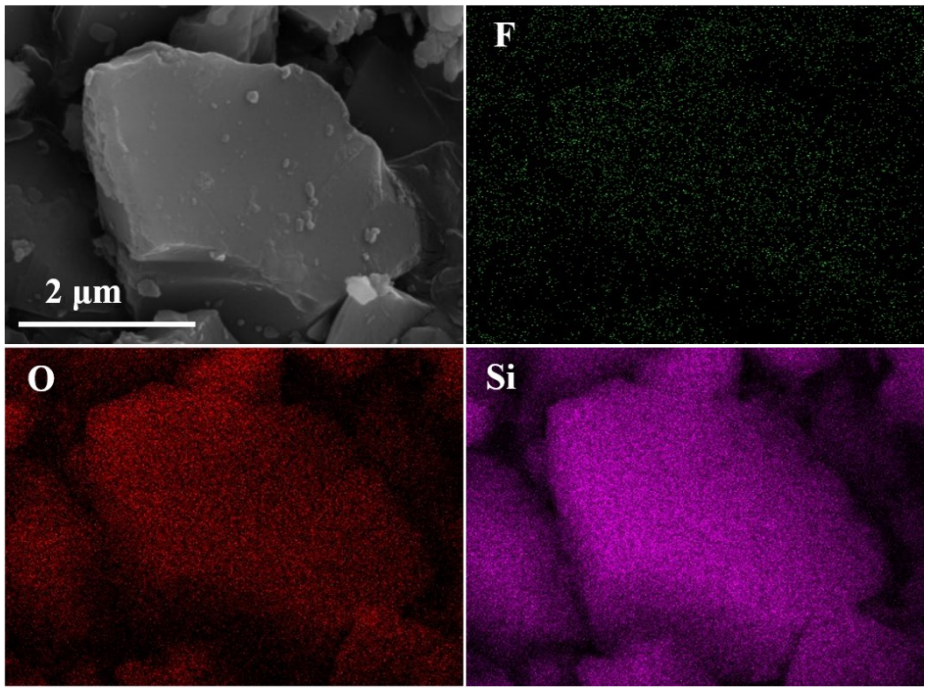

Figure S2. SEM images and corresponding element mappings of Si, O and F in SiOG@LiF3.

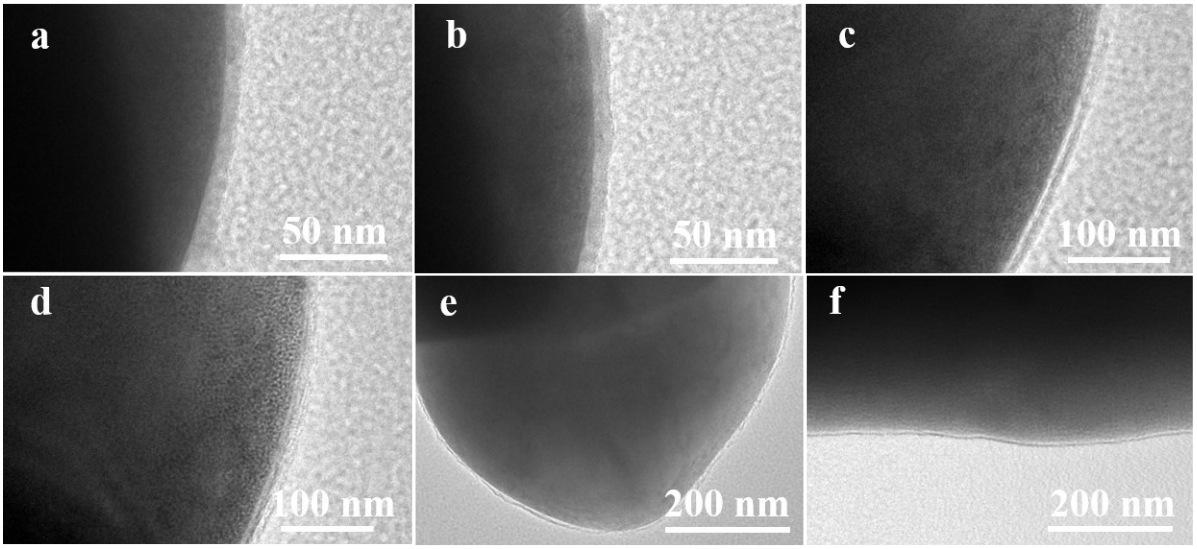

Figure S3. TEM images of SiOG@LiF3 at different magnifications.

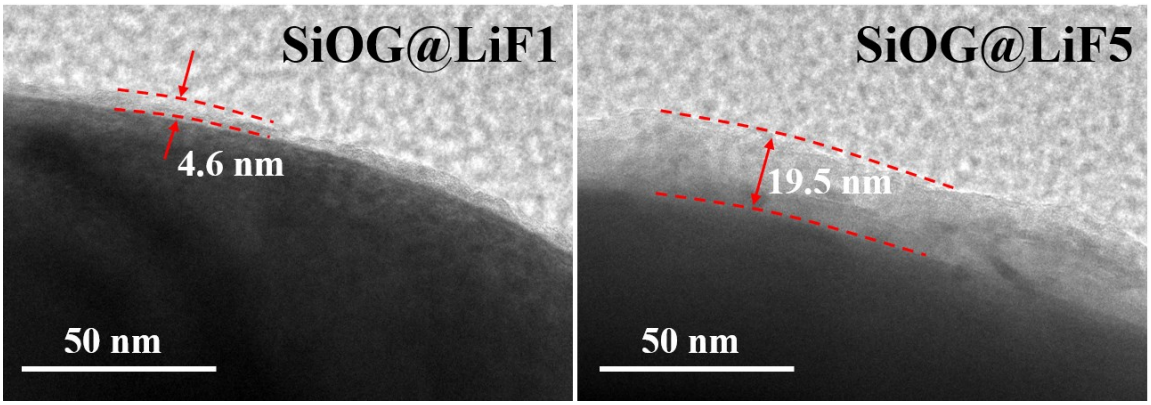

Figure S4. TEM images of SiOG@LiF1 and SiOG@LiF5.

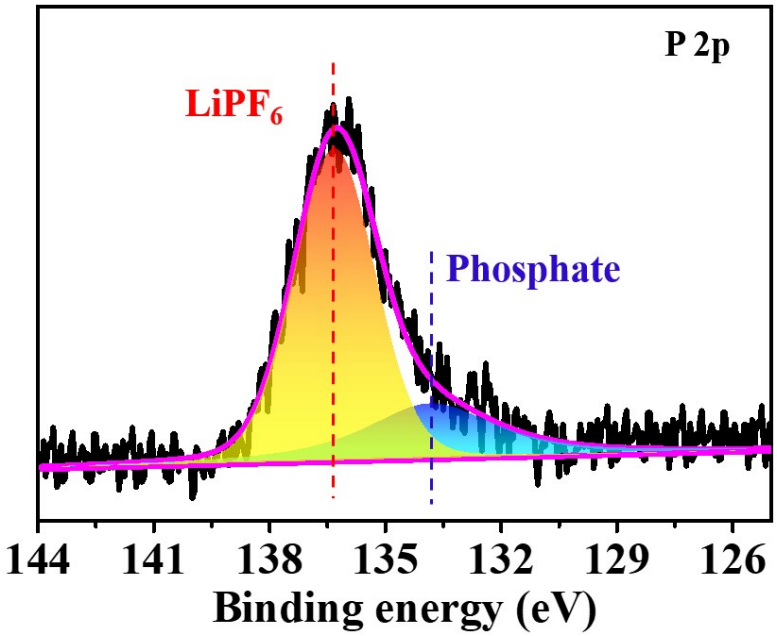

Figure S5. High resolution P 2p of sample SiOG@LiF3 after heating.

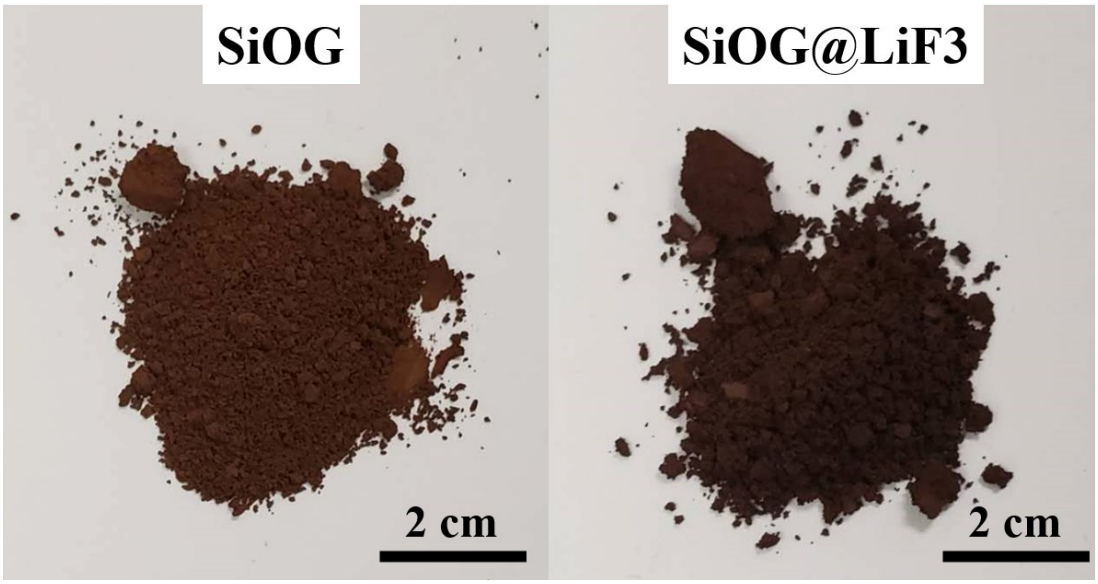

Figure S6. Digital images of SiOG and SiOG@LiF3 powder.

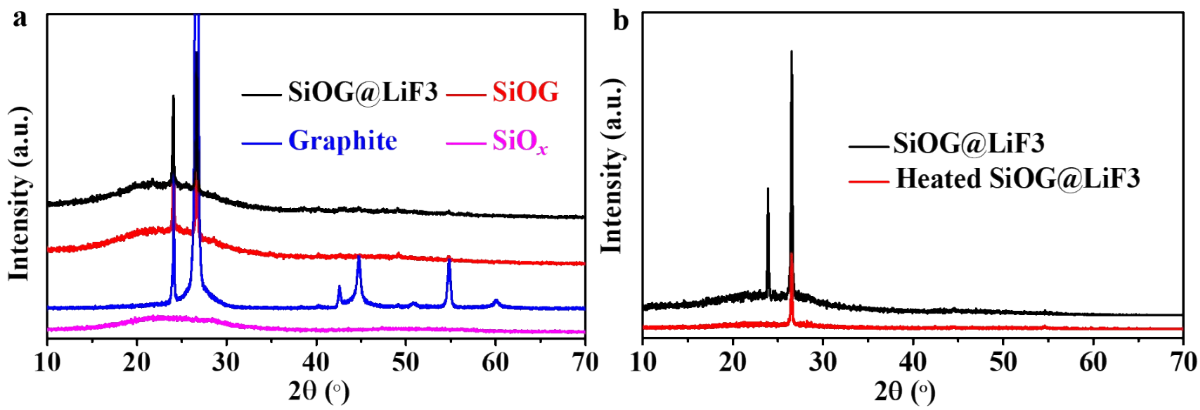

Figure S7. (a) XRD pattern of SiO_x, graphite, SiOG and SiOG@LiF3. (b) XRD patterns of SiOG@LiF3 before and after heating.

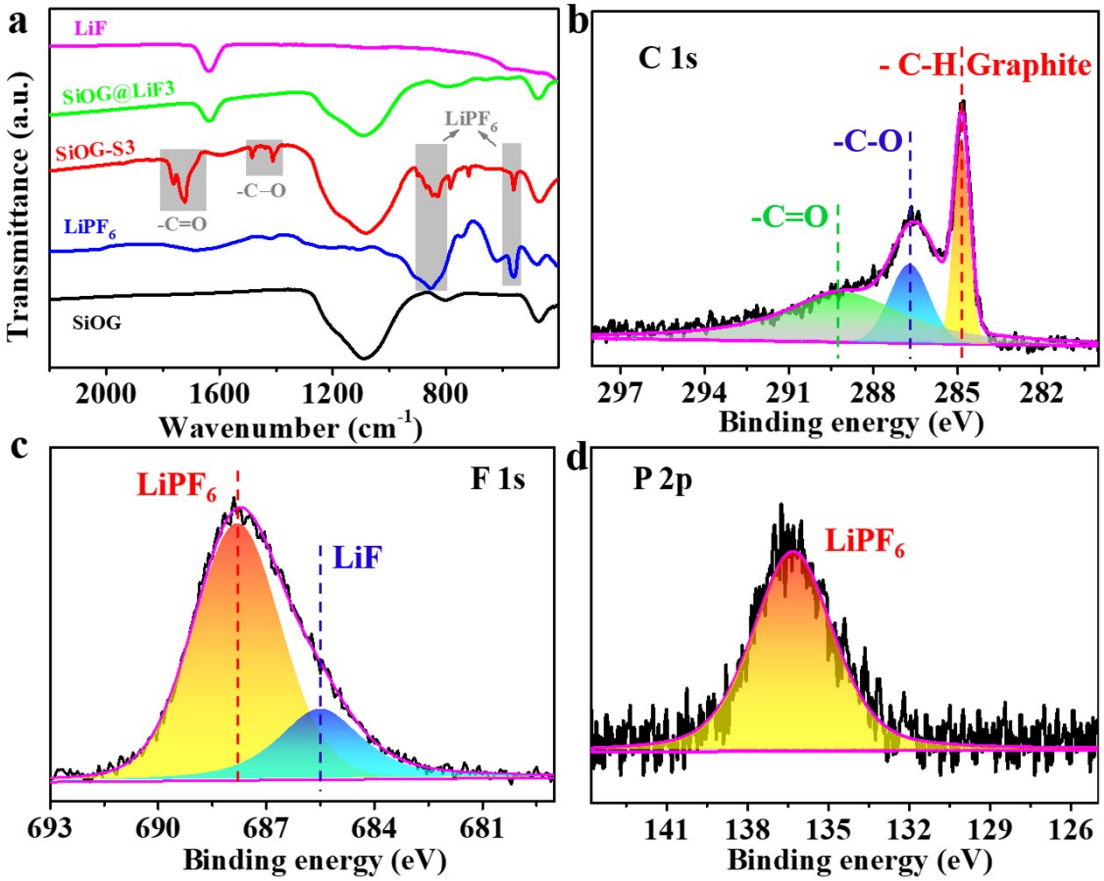

Figure S8. (a) FTIR results of samples LiF, SiOG@LiF3, SiOG-S3, $LiPF_6$ and SiOG; (b, c, d) C 1s, F 1s and P 2p of sample SiOG-S3.

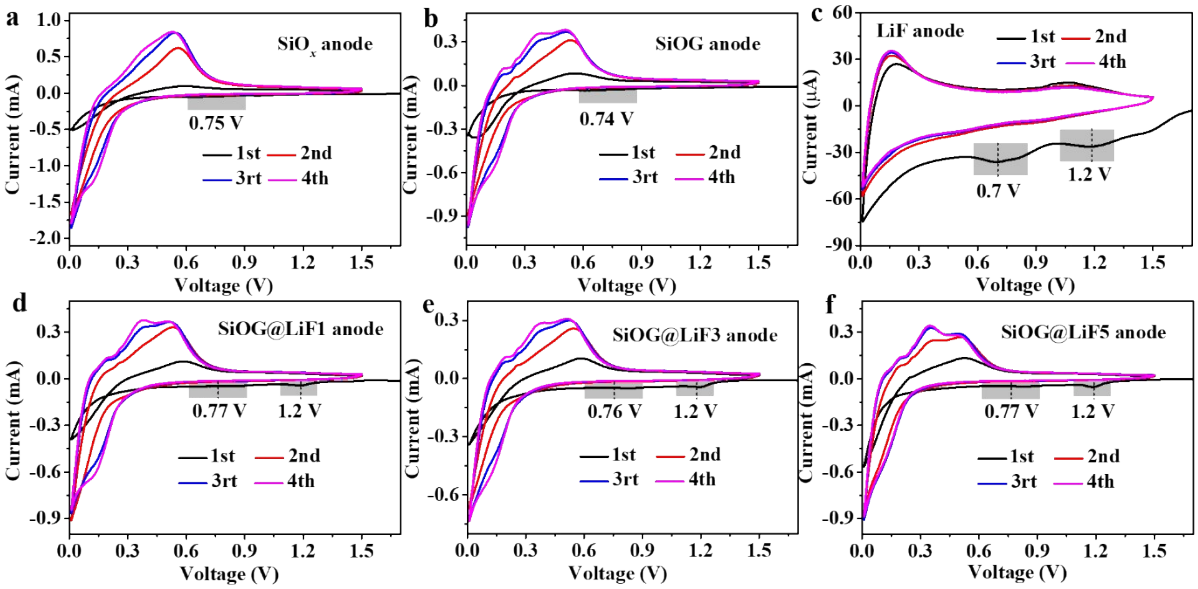

Figure S9. CV curves of (a) SiO_x, (b) SiOG, (c) LiF anode, (d) SiOG@LiF1, (e) SiOG@LiF3 and (f) SiOG@LiF5. The scan rate is 0.1 mV s^{-1}.

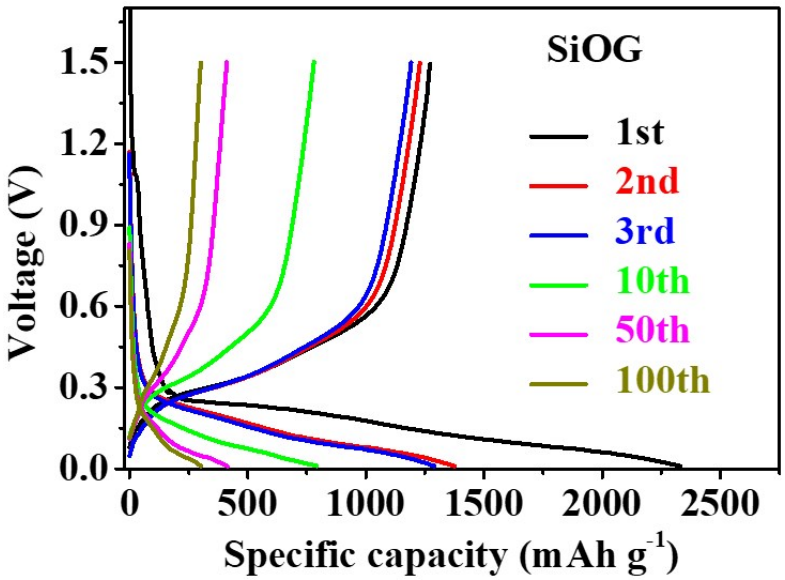

Figure S10. Typical charge/discharge profiles of sample SiOG under 500 mA g^{-1} and 100 mA g^{-1} for the first three cycles.

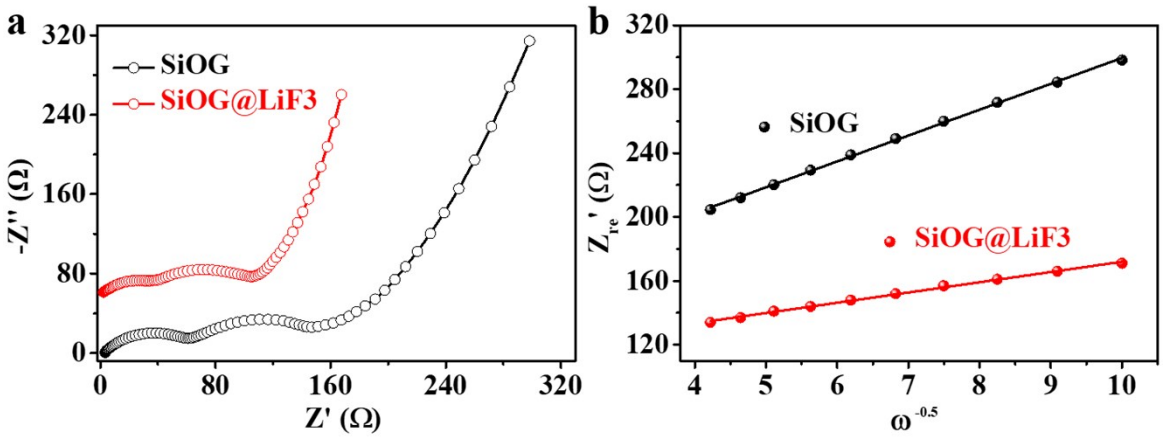

Figure S11. (a) Nyquist plots of SiOG and SiOG@LiF3 electrodes after 1cycle. (b) Linear relationship between real impedance and reciprocal square root of low-angular frequency.

The lithium ion diffusion coefficient (D_{Li}^+) can be calculated according to the equations ($Z_{re} = R_e + R_f + R_{ct} + \sigma_w\omega^{-0.5}$; $D_{Li}^+ = 0.5(RT/AF^2\sigma_wC)^2$), where *R, T, A, F,* and *C* are gas constant, absolute temperature, surface area of electrode, Faraday constant and the concentration of lithium ion, respectively.[1] Figure S8a and S8b shows the Nyquist plots of SiOG and SiOG@LiF3 electrodes after 1cycle and corresponding linear relationship between Z_{re}' and $\omega^{-0.5}$ where the Warburg coefficient σ_w can be derived according to above equations. Therefore, the calculated D_{Li}^+ of SiOG and SiOG@LiF3 after 1 cycle are 7.28×10^{-14} and 5.38×10^{-13} cm^2 s^{-1} respectively.

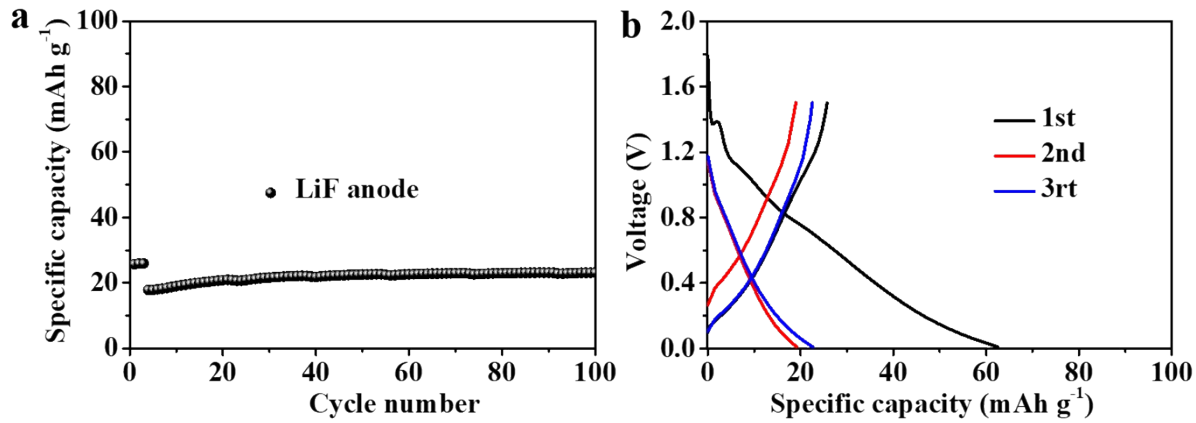

Figure S12. Cycling stability (a) and typical charge/discharge profiles (b) of LiF anode under 500 mA g^{-1} and 100 mA g^{-1} for the first three cycles.

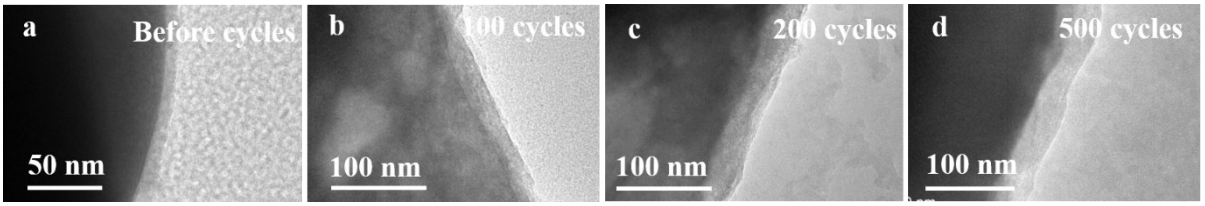

Figure S13. (a-d) TEM images of SiOG@LiF3 sample before cycle, after 100 cycles, 200 cycles and 500 cycles.

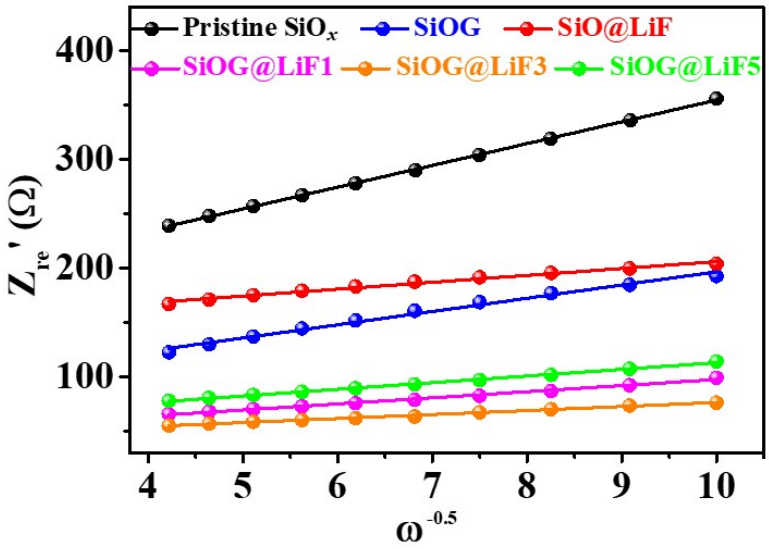

Figure S14. Linear relationship between real impedance and reciprocal square root of low-angular frequency.

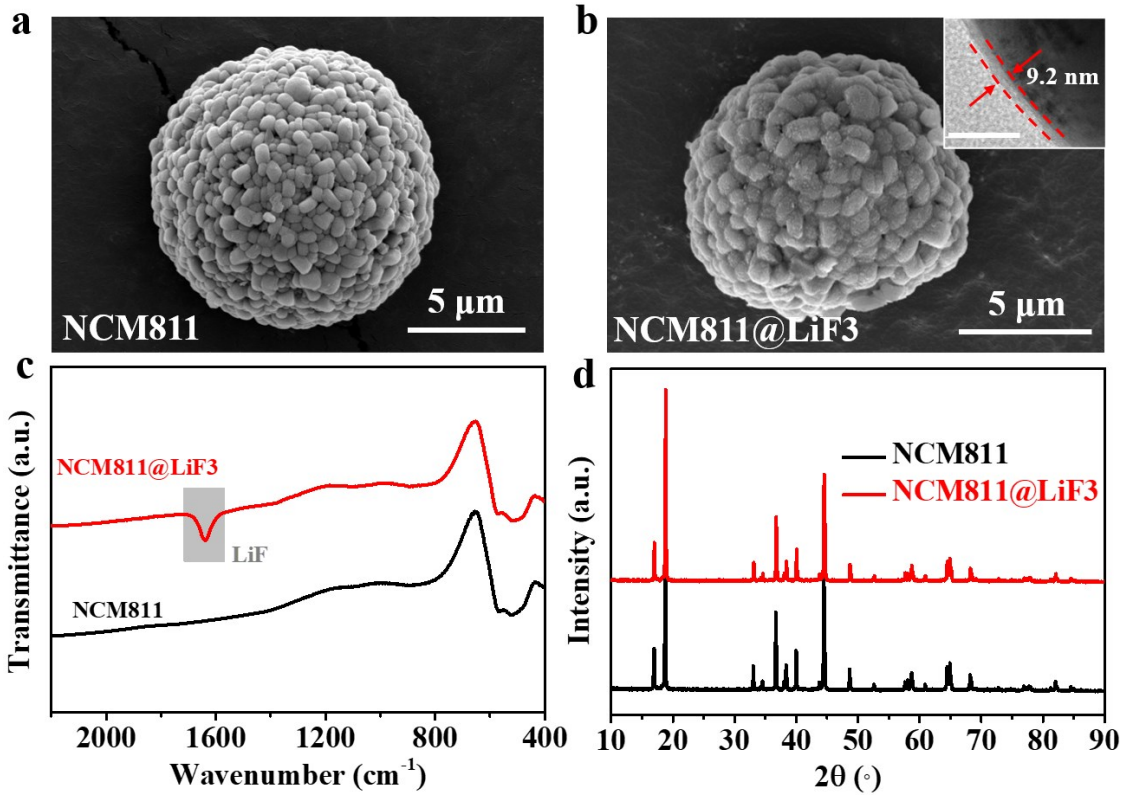

Figure S15. SEM images (a, b), FTIR spectrum (c) and XRD patterns (d) of NCM811 and NCM811@LiF3. The inset in Figure S6b is a TEM image of NCM811@LiF3 and the scale bar is 50 μm.

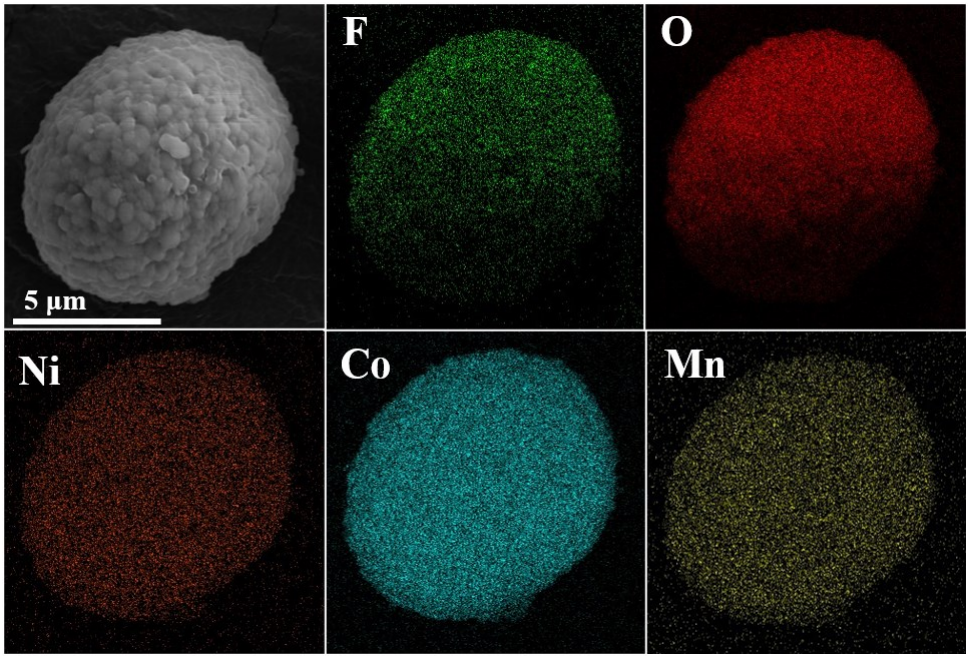

Figure S16. SEM images and corresponding element mappings of F, O, Ni, Co and Mn in NCM811@LiF3.

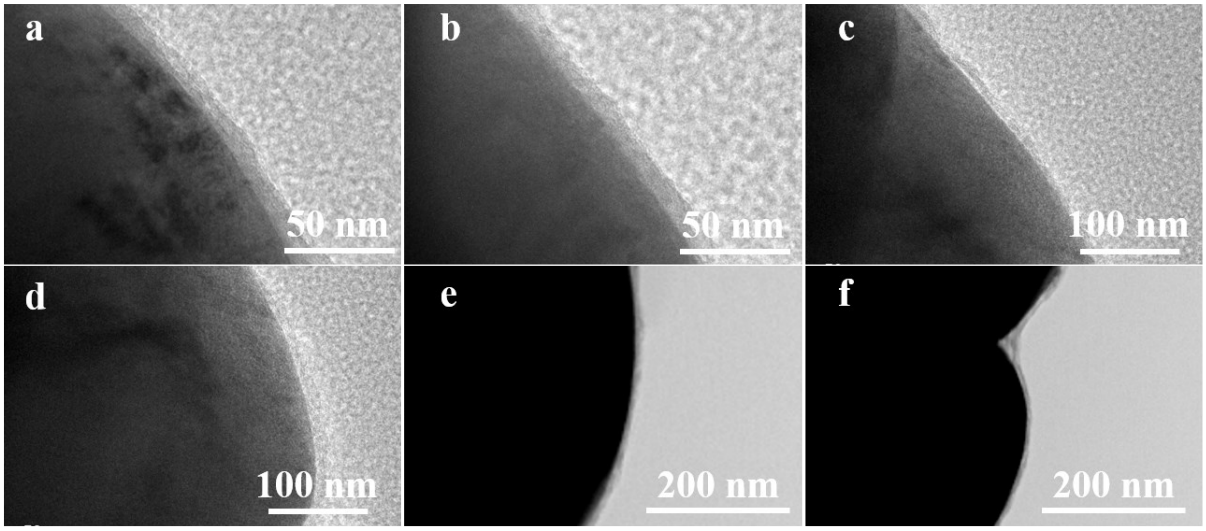

Figure S17. TEM images of NCM811@LiF3 at different magnifications.

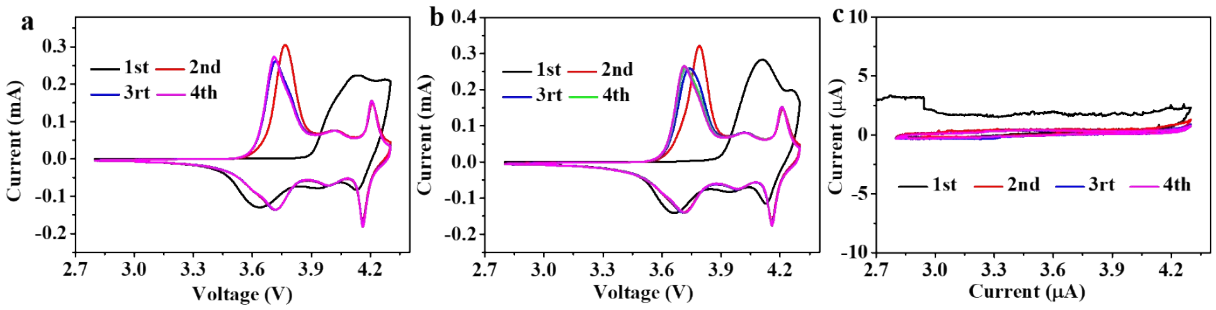

Figure S18. CV curves of (a) NCM811, (b) NCM811@LiF3 and (c) LiF cathode. The scan rate is 0.1 mV s^{-1}.

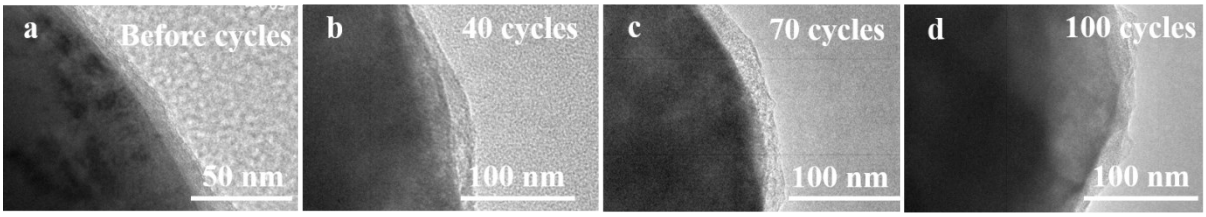

Figure S19. (a-d) TEM images of NCM811@LiF3 sample before cycling, after 40, 70 and 100 cycles.

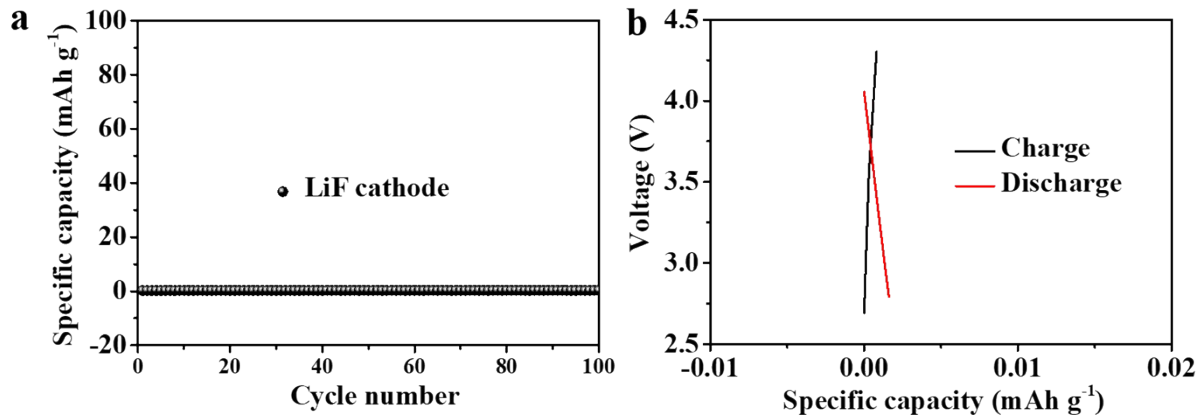

Figure S20. Cycling stability (a) and typical charge/discharge profiles (b) of LiF cathode under 100 mA g^{-1}.

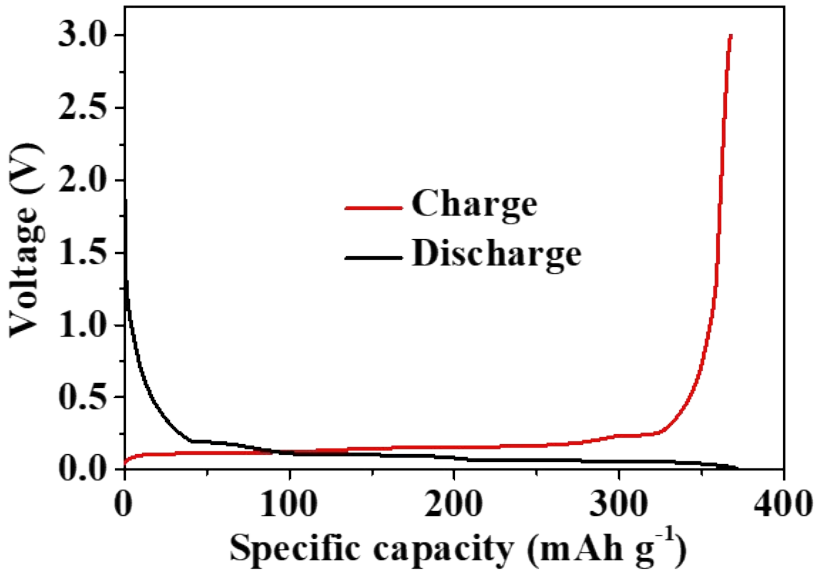

Figure S21. The 1st charge/discharge curves of graphite anode.

Note 1. The portion of SiO_x of whole SiO_x joined in the electrochemical events can be calculated as the equation: $P = D_a/D_t$, where P is the portion of SiO_x of whole SiO_x joined in the electrochemical events, D_a is the actual initial discharge capacity of SiO_x in SiOG@LiF3 anode, D_t is the theoretical specific capacity of SiO_x (~ 2680 mAh g^{-1} [12]). The 1st discharge capacity of SiOG@LiF3 anode is 2065 mAh g^{-1}, and 1st discharge capacity of graphite anode is 371 mAh g^{-1}. Given that the content of graphite in SiOG sample is 10 wt% (the corresponding SiO_x content is 90%), D_a of SiOG@LiF3 anode is 2253 mAh g^{-1} ((2065-371*10%)/90%). Therefore, the calculated P of SiOG@LiF3 anode is 84.1%, which means about 84.1% of whole SiO_x joined the electrochemical events. Note that the capacity contribution of LiF can be ignored due to its low capacity (Figure S12) and low content.

Table S1. Comparison of the rate performance between SiO_x-based materials reported recently.

Materials	Current density (mA g^{-1})	Capacity (mAh g^{-1})	Ref.
SiO_x/C-2	200	792	2
	600	620	
Sn_2Fe@30SiO_x	200	710	3
	2000	570	
SiO_x/G/C	300	750	4
	3000	592	
SiO_x–TiO2@C	200	916	1
	3200	542	
SiO_x/C	325	645	5
	3250	549	
SiO_x/TiO_2@MLG	200	1052	6
	5000	429	
SiO_x/C-CVD	200	1120	7
	5000	410	
SiO_x@C	200	1117	8
	5000	426	
SiO_x@G	500	1100	9
	5000	795	
C-SiO_x/C	300	1410	10
	7500	1191	
SiO_x@TiO_2@C	500	1440	11
	5000	1146	
SiOG@LiF3	200	1276	This work
	5000	741	

Table S2. Combined interfacial resistance and D_{Li}^{+} of pristine SiO_x, SiO@LiF3, SiOG, SiOG@LiF1, SiOG@LiF3 and SiOG@LiF5 after 100 cycles

Samples	Pristine SiO_x	SiO@LiF3	SiOG	SiOG@LiF1	SiOG@LiF3	SiOG@LiF5
***R*1 (Ω)**	103.93	56.48	38.25	15.89	13.84	16.55
***R*2 (Ω)**	133.25	69.26	40.77	22.75	16.28	35.38
Combined interfacial resistance	237.18	125.74	79.02	38.64	30.12	51.93
$D_{Li}^{+} \times 10^{-13}$ ($cm^2\ s^{-1}$)	0.58	5.8	0.89	7.3	9.13	7.42

Table S3. Calculated HOMO/LUMO energy levels and energy gap of electrolyte compounds (EC, EC, DMC, FEC and $LiPF_6$)

Samples		EMC	EC	DMC	FEC	$LiPF_6$
Energy (eV)	**LUMO**	1.21	1.07	1.15	0.52	-1.61
	HOMO	-7.63	-8.02	-7.70	-8.44	-10.01
GAP (eV)		8.84	9.09	8.85	8.96	8.40

References

1. Z. Li, H. Zhao, P. Lv, Z. Zhang, Y. Zhang, Z. Du, Y. Teng, L. Zhao and Z. Zhu, *Adv. Funct. Mater.*, 2018, **28**, 1605711.
2. Z. Liu, D. Guan, Q. Yu, L. Xu, Z. Zhuang, T. Zhu, D. Zhao, L. Zhou and L. Mai, *Energy Storage Materials*, 2018, **13**, 112-118.
3. H. Zhang, R. Hu, Y. Liu, X. Cheng, J. Liu, Z. Lu, M. Zeng, L. Yang, J. Liu and M. Zhu, *Energy Storage Materials*, 2018, **13**, 257-266.
4. G. Li, J.Y. Li, F.S. Yue, Q. Xu, T.T. Zuo, Y.X. Yin and Y.G. Guo, *Nano Energy*, 2019, **60**, 485-492.
5. Q. Xu, J.K. Sun, Y.X. Yin and Y.G. Guo, *Adv. Funct. Mater.*, 2018, **28**, 1705235.
6. H. Xue, Y. Wu, Y. Zou, Y. Shen, G. Liu, Q. Li, D. Yin, L. Wang and J. Ming, *Adv. Funct. Mater.*, 2020, **30**, 1910657.
7. Z. Liu, Y. Zhao, R. He, W. Luo, J. Meng, Q. Yu, D. Zhao, L. Zhou and L. Mai, *Energy Storage Materials*, 2019, **19**, 299-305.
8. Z. Li, H. Zhao, J. Wang, T. Zhang, B. Fu, Z. Zhang and X. Tao, *Nano Res.*, 2020, **13**, 527-532.
9. Q. Xu, J. K. Sun, Z. L. Yu, Y. X. Yin, S. Xin, S. H. Yu and Y. G. Guo, *Adv. Mater.*, 2018, **30**, 1707430.
10. G. Li, L.B. Huang, M.Y. Yan, J.Y. Li, K.C. Jiang, Y.X. Yin, S. Xin, Q. Xu and Y.G. Guo, *Nano Energy*, 2020, **74**, 104890.
11. Z. Xiao, C. Yu, X. Lin, X. Chen, C. Zhang, H. Jiang, R. Zhang and F. Wei, *Nano Energy*, 2020, **77**, 105082.
12. D. He, P. Li, W. A. Wang, Q. Wan, J. Zhang, K. Xi, X. Ma, Z. Liu, L. Zhang and X. Qu, *Small*, 2020, 16, 1905736.